Crystallographic orientation of silicon on an amorphous substrate using an artificial surface-relief grating and laser crystallization

M. W. Geis, D. C. Flanders, and Henry I. Smith

Citation: Applied Physics Letters **35**, 71 (1979); doi: 10.1063/1.90936
View online: http://dx.doi.org/10.1063/1.90936
View Table of Contents: http://scitation.aip.org/content/aip/journal/apl/35/1?ver=pdfcov
Published by the AIP Publishing

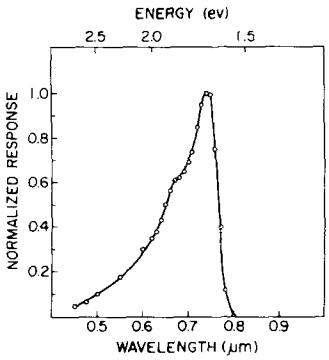

FIG. 2. Spectral response for a front-illuminated Cu/$CuGaSe_2$ cell at room temperature.

cells. The value of the built-in potential, obtained from these measurements when adjusted for the Fermi level of the semiconductor, is in agreement with the barrier height calculated from I-V data.

In the optimum cells, a crossover effect between the dark and light I-V curves was observed. This may be evidence of the existence of an additional photoconductive layer. We believe it to be p-type $CuGaSe_2$ compensated by the diffusion of copper. A similar effect was observed in CdS-Cu_2S cells.[4]

Figure 2 shows the photoresponse (I_{sc}) for a front-illuminated Cu/$CuGaSe_2$ cell as a function of wavelength. The low response in the short-wavelength region is most likely due to the high density of the interface states. This conclusion is supported by the measured value of the barrier height (0.6 V), which is roughly equal to one-third of the band gap of $CuGaSe_2$. This is considered to be valid when the surface-state density on the semiconductor surface is large.

This research has been partially supported by Consejo Nacional de Investigaciones Científicas y Tecnológicas (CONICIT). The authors would like to thank Dr. N. Bottka for valuable suggestions and L. Videla for technical assistance.

[1]J.L. Shay and J.H. Wernick, in *Ternary Chalcopyrite Semiconductors: Growth, Electronic Properties and Application* (Pergamon, New York, 1975), p. 188.
[2]J.J. Loferski, J. Appl. Phys. **27**, 777 (1956).
[3]S.M. Sze, *Physics of Semiconductor Devices* (Wiley-Interscience, New York, 1969), p. 395.
[4]B.G. Caswell, G.J. Russell, and J. Woods. J. Phys. D **8**, 1889 (1975).

Crystallographic orientation of silicon on an amorphous substrate using an artificial surface-relief grating and laser crystallization

M. W. Geis, D. C. Flanders, and Henry I. Smith[a)]
Lincoln Laboratory, Massachusetts Institute of Technology, Lexington, Massachusetts 02173

(Received 22 January 1979; accepted for publications 20 April 1979)

Uniform crystallographic orientation of silicon films, 500 nm thick, has been achieved on amorphous fused-silica substrates by laser crystallization of amorphous silicon deposited over surface-relief gratings etched into the substrates. The gratings had a square-wave cross section with a 3.8-μm spatial period and a 100-nm depth. The ⟨100⟩ directions in the silicon were parallel to the grating and perpendicular to the substrate plane. We propose that orientation of overlayer films induced by artificial surface patterns be called graphoepitaxy.

PACS numbers: 68.55. + b, 61.50.Cj, 81.10. − h, 85.40.Ci

In earlier work, surface-relief gratings with square-wave cross section in amorphous SiO_2 were used to induce oriented growth of KCl crystallites grown from a water solution [1] and to align overlayer films of nematic and smectic A liquid crystals.[2,3] The authors speculated that control of overlayer crystallographic orientation by means of artificial surface-relief structure should be applicable to a broad range of overlayer/substrate combinations and deposition methods.[1–5] Here, we report uniform crystallographic orientation of thin silicon films on amorphous fused-silica substrates, achieved by laser crystallization of amorphous silicon deposited over a surface-relief grating in the substrate. We propose that such examples of orientation induced by artificial surface patterns be called "graphoepitaxy".[6]

A theoretical model[4] predicts that film-formation methods that yield textured polycrystalline films (i.e., the individual crystal grains have one particular plane parallel to the substrate surface and random orientation otherwise) on smooth amorphous substrates should yield uniformly oriented films if such film formation is carried out over an appropriate surface-relief structure in the amorphous substrate. For example, polycrystalline films with (100) texture [i.e., (100) planes of grains are parallel to the substrate surface, but orientation is random in the surface plane] should become uniformly oriented on a surface-relief grating with square-wave cross section if the spatial period of the grating is small compared to the normal grain size. Specifically, the

[a)]Also, Department of Electrical Engineering and Computer Science, Massachusetts Institute of Technology, Cambridge, Mass. 02139.

 0003-6951/79/010071-04$00.50

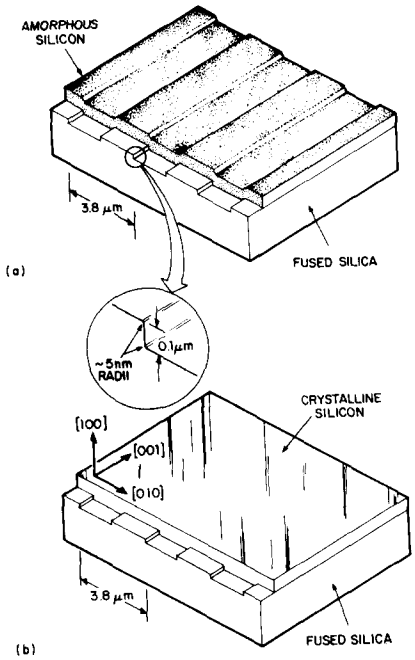

FIG. 1. Schematic illustration of (a) an amorphous silicon film deposited by a CVD process over a surface-relief grating in fused silica; (b) a uniformly oriented film of silicon obtained by laser crystallization of the amorphous silicon over the relief structure. Note that in (b) the top surface of the silicon does not follow the contour of the grating, as in (a). In practice, the surface of the silicon in (b) has a roughness of several 10 nm.

model, which is based on equilibrium thermodynamics, states that such uniform orientation is a configuration of minimum free energy. Polycrystalline films of (111) texture, on the other hand, would require a relief structure having facets that intersect at 70.5° and/or 109.5°. Relief structures with square-wave cross section are more easily fabricated using current techniques, [4,7,8] and thus one is led to seek film-formation methods that yield (100) or (110) textured silicon. It is known that laser crystallization of silicon films yields grains several micrometers in diameter. [9,10] We found that under certain conditions laser crystallization of amorphous silicon over fused silica yields a nearly perfect (100) texture.

Several experiments were performed to determine the texture of laser-crystallized amorphous and polycrystalline silicon, deposited by a variety of methods, on optically polished fused-silica substrates. In some cases the polished fused silica was coated with SiO_2 deposited by a CVD process. With amorphous silicon films 500 nm thick, deposited at 610 °C in a commercial CVD reactor [11] using the reaction $SiH_4 \xrightarrow{N_2} Si + 2H_2$, we were able to obtain 100% of a (100) texture after laser crystallization, as determined by x-ray diffractometry. The maximum deviation of (100) from the substrate plane was about 3°, as determined by reflection electron diffraction (RED). With silicon deposited by thermal evaporation and by the reaction $SiH_4 \rightarrow Si + 2H_2$ in a low-pressure CVD reactor, [11] we observed 100% (111) and relatively weak (100) textures, respectively. The laser crystallization was done in air at room temperature using an argon-ion laser, operating multiline at a power level between 6 and 7 W and focused with a 60-mm focal-length lens placed 45 mm from the silicon film. For a single linear scan, this beam produced a band of crystallization about 380 μm wide. Samples were scanned past the beam at 10 mm/sec or slower, in a raster fashion, with successive horizontal scans stepped vertically by 12 μm. After multiple raster scans of a silicon film in the laser beam, polycrystalline grains grew to 10–100 μm in diameter, indicating that uniform crystallographic orientation should be obtainable with square-wave gratings having spatial periods of several micrometers.

To obtain square-wave gratings in fused-silica substrates we first coated the substrates with a film of chromium 20 nm thick. Using conformable photomask lithography, [12] a 3.8-μm spatial-period grating was then exposed and developed in AZ1350B photoresist, [13] and the chromium etched in a chemical etchant. After removal of the photoresist, a square-wave grating was etched into the fused silica by reac-

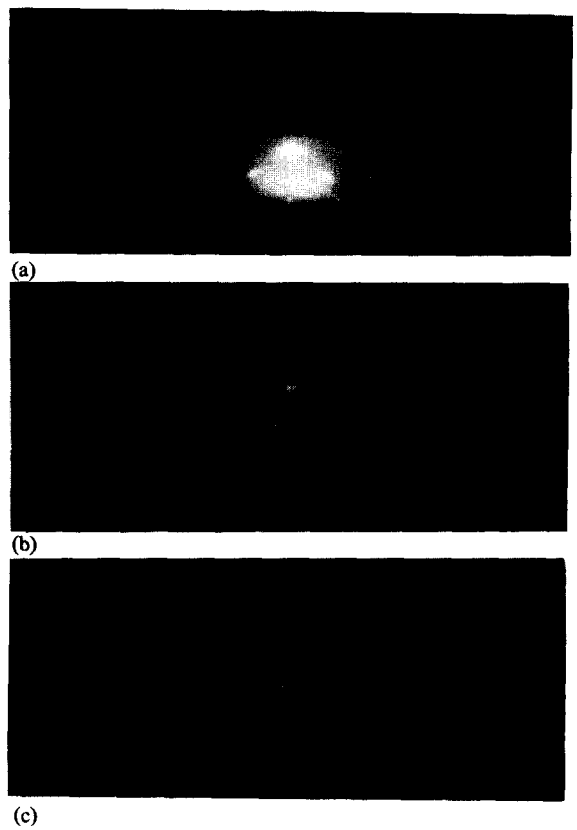

FIG. 2. (a) Reflection electron diffraction pattern showing the (100) texture of a laser-crystallized silicon film on a smooth amorphous fused-silica substrate. The length of the arcs in the pattern indicates that the maximum deviation of the (100) planes from parallel with the substrate is about 3°. The pattern is independent of rotation about the substrate normal, indicating absence of any in-plane orientation. (b) Reflection electron diffraction pattern of a silicon film laser crystallized over a 3.8-μm spatial period, 100 nm deep, square-wave grating in amorphous fused silica. The electron beam is parallel to the grating lines. The observed (100) pattern indicates uniformly oriented silicon having $<100>$ directions parallel to the grating lines and perpendicular to the substrate surface. (c) Reflection electron diffraction pattern of the same sample as in (b) but with the electron beam at 45° to the grating lines. The diffraction pattern is (110). The appearance of arcs rather than spots in (b) and (c) indicates that the film consists of sigle-crystal regions where the (100) plane deviates a maximum of about 3° with respect to the substrate surface.

FIG. 3. Transmission electron diffraction pattern of a 500-nm-thick silicon film laser crystallized over a 3.8-μm period square-wave grating in amorphous fused silica. The electron beam was perpendicular to the silicon film yielding a (100) diffraction pattern. The Kikuchi lines visible in the pattern indicate a high degree of crystalline perfection.

tive-ion etching in CHF_3 gas using the chromium grating as a mask.[4,7,8] Finally, the chromium was removed in a chemical etchant. This procedure yields square-wave gratings with flat tops, flat bottoms, and sidewalls that deviate a maximum of about 6° from the vertical. The radii of curvature at the corners where the sidewalls join the tops and groove bottoms are about 5 nm. The deviation of a sidewall from an ideal planar facet depends primarily on the edge ripple in the original photomask and any additional smoothing or roughening that occurs during the chemical etching of the chromium. Typically, the deviation is about $\pm$ 100 nm. In the experiments reported here groove depths were 19, 60, and 100 nm. Substrates were cleaned just prior to depositing silicon on them, the final cleaning step being irradiation for about 40 min in air with a far-uv lamp.[14] The lamp generates ozone and is very effective in removing any residual organic contamination.

For the crystallographic orientation experiments about 500 nm of amorphous silicon was deposited by the CVD process,[11] referred to above, over fused-silica substrates 1.5 mm thick and 38 mm in diameter. The 3.8-μm spatial-period grating was 100 nm deep and covered a square area about 15 mm on a side. The silicon was laser crystallized, both inside and outside the grating area, using the scanning procedure described above, at laser powers of 6 and 7 W. After a single raster scan at 6 W the amorphous silicon became polycrystalline, with (100) texture and grains 10–20 μm in diameter, but no orientation relative to the grating was measurable. After a second raster scan, grains had grown to about 100 μm in diameter, and there was a definite preferred orientation relative to the grating as determined by RED. After four raster scans, a nearly perfect orientation relative to the grating was obtained, where the $<100>$ directions in the silicon are parallel to the grating and perpendicular to the substrate surface, as illustrated schematically in Fig. 1(b). To verify that the grating geometry, and not the direction of the laser scan, determines the silicon orientation, scans were made parallel, perpendicular and at 45° to the grating. Orientation was found to be independent of laser scan direction. As depicted in Fig. 1(a), the deposit of amorphous silicon conforms to the contour of the underlying grating. With laser crystallization, however, there is substantial redistribution of material: the top surface of the silicon becomes roughened, but it is generally planar with no evidence of even a shallow grating. Outside the grating area the film consists of single-crystal grains, 10–100 μm in diameter, that have a (100) texture, with random orientation in the plane of the substrate. Figure 2 shows a comparison of the RED patterns obtained inside and outside the grating area. The small arcs in Fig. 2 indicate a slight deviation of (100) texture from one area in the film to another. Such deviation is present both inside and outside the grating area.

Figure 3 shows a transmission diffraction pattern taken in a transmission electron microscope of a silicon film laser crystallized over the grating. The silicon was separated from the fused-silica substrate by immersion in a HF solution. The Kikuchi lines in the diffraction pattern indicate a highly ordered crystalline structure.[15]

If the laser power is increased to 7 W, grains having a variety of shapes up to 200 μm in diameter form on the first raster scan, but no crystallographic orientation is observed in the grating area. This absence of orientation persists despite repeated scans. Removal of the silicon in hydrazine indicates some damage to the grating at the 7-W power level. Also, at 7 W the silicon appears to be melted by the laser irradiation.

The cross-sectional profile of the grating plays an important role in controlling crystallographic orientation. If the depth of the grating is reduced to 60 nm, the crystallographic orientation degrades somewhat, and at a depth of 19 nm no evidence of orientation relative to the grating is observed by RED. If the bottom corners of the grating are rounded to a radius of curvature of about 80 nm, the orientation effect of the grating is substantially degraded. This is understandable qualitatively from the theoretical model,[4] and is in agreement with similar results obtained with KCl where orientation would not occur on gratings with rounded corners.[4]

We have demonstrated uniform crystallographic orientation of silicon films on amorphous fused-silica substrates, achieved by laser crystallization over a surface-relief grating with square-wave cross section. This opens the possibility of new methods of preparing films for microelectronic devices and solar cells.

The authors are grateful to R.A. Reynolds for encouraging the use of laser crystallization, J.C.C. Fan for helpful discussions on laser crystallization, H.P. Jensen for the use of his argon laser, M.I. Naiman and T.O. Herndon for use of their scanning apparatus, and N. Efremow, P.D. DeGraff, F.C. Chimi, R.C. Hartford, C.L. Doherty, and C.A. Smith for their skillful technical assistance. This work was sponsored by the Defense Advanced Research Projects Agency.

[1]H.I. Smith and D.C. Flanders, Appl. Phys. Lett. **32**, 349 (1978).
[2]H.I. Smith, D.C. Flanders, and D.C. Shaver, in *Scanning Electron Microscopy*, Vol. 1, edited by Om Johari (Scanning Electron Microscopy, Inc., AMF O'Hare, Ill. 60666, 1978), pp. 33–40.
[3]D.C. Flanders, D.C. Shaver, and H.I. Smith, Appl. Phys. Lett. **32**, 597 (1978).

[4]D.C. Flanders, Ph.D. thesis (M.I.T., 1978); reprinted as M.I.T. Lincoln Laboratory Technical Report 533, 1978.
[5]D.C. Flanders and H.I. Smith, J. Vac. Sci. Technol. **15**, 1001 (1978).
[6]From the greek: grapho—to write or incise; epi—upon; taxis—arrangement, order.
[7]D.C. Flanders, H.I. Smith, H.W. Lehmann, R. Widmer, and D.C. Shaver, Appl. Phys. Lett. **32**, 112 (1978).
[8]H.W. Lehmann and R. Widmer, Appl. Phys. Lett. **32**, 163 (1978); Appl. Phys. Lett. **33**, 367 (1978) (erratum).
[9]J.C.C. Fan and H.Z. Zeiger, Appl. Phys. Lett. **27**, 224 (1975).
[10]A. Gat, L. Gerzberg, J.F. Gibbons, T.J. Magee, J. Peng, and J.D. Hong, Appl. Phys. Lett. **33**, 775 (1978).
[11]General Signal/Tempress, Sunnyvale, Calif.
[12]J. Melngailis, H.I. Smith, and N. Efremow, IEEE Trans. Electron Devices ED-**22**, 496 (1975).
[13]Shipley Company, Newton, Mass.
[14]John R. Vig, IEEE Trans. Parts, Hybrids, and Packag. PHP-**12**, 365 (1976).
[15]R.P. Heidenreich, *Fundamentals of Transmission Electron Microscopy* (Interscience, New York, 1964), Chap. 3.

Planar guarded avalanche diodes in InP fabricated by ion implantation

J. P. Donnelly, C. A. Armiento, V. Diadiuk, and S. H. Groves
Lincoln Laboratory, Massachusetts Institute of Technology, Lexington, Massachusetts 02173

(Received 22 February 1979; accepted for publication 26 April 1979)

Planar guarded avalanche diodes in InP have been fabricated using a double-ion-implantation technique. Silicon was selectively implanted into an n-type epitaxial layer to increase the concentration in the central portion of the diode, and beryllium was implanted to form the p-n junction. When appropriately reverse biased, these diodes exhibited uniform avalanche photocurrent gain in the central portion, where the electric field is maximum. With a 1-kΩ load, photoresponse gains as high as 20 were measured, although values of 6 to 8 were more typical. At present, the external photoresponse gain with a fixed load is limited by the shunting effect of the diode's differential resistance.

PACS numbers: 61.70.Tm, 85.60.Gz, 85.30.Mn

There is currently a great deal of interest in avalanche photodiodes [1–5] and IMPATT diodes [6] in InP and $In_{1-x}Ga_xAs_yP_{1-y}$. To date, all of the avalanche diodes reported in these materials have relied on etched mesa and/or punch-through p-n junction structures to reduce the problem of edge breakdown. In this letter, we present some initial results on a planar guarded avalanche structure in InP fabricated using a double-ion-implanation technique. The structure is similar to that used in guarded reach-through Si diodes, [7,8] and, in addition to its value in preventing edge breakdown, can in the future be tailored to optimize the electric field profile for maximum avalanche gain and/or high carrier-collection efficiency. The results presented in this letter represent the first successful implantation of more than one atomic species in InP and should therefore serve to indicate the extent to which ion implantation can now be used in InP device fabrication. In addition, prevous results [5,9] indicate that the ion-implantation techniques reported here are directly transferable to the $In_{1-x}Ga_xAs_yP_{1-y}$ system for longer-wavelength operation.

Figure 1 illustrates schematically a cross section of a guarded InP p-n junction diode. Viewed from the top, the p^+ and n regions would appear as concentric circles. By appropriately selecting the carrier concentration n and the thickness t of the n-type region (in relation to the concentration in n^- region), the maximum electric field at breakdown in the central region can be made larger than the electric field at the edge of the p^+ region. Under this condition, avalanche breakdown will occur in the central portion of the diode and not at the edge. The minimum nt product necessary to prevent edge breakdown depends on both the concentration in the n^- region and the shape of the p^+-n^- boundary at the periphery. For initial design purposes, the maximum field at the edge of an implanted 0.3-μm-deep p-n junction due to field crowding was estimated to be about twice that in the flat portion of the junction. [10]

The InP samples used in this work consisted of an unintentionally doped n-type epitaxial layer (n^- region of Fig. 1) with an electron concentration of $(1–2)\times 10^{16}$ cm^{-3} grown by liquid phase epitaxy on a (100)-oriented n^+-InP substrate. The thickness of the epilayer is not critical but was chosen to be greater than 6 μm to prevent punch-through, which would somewhat negate the guarding properties of this structure.

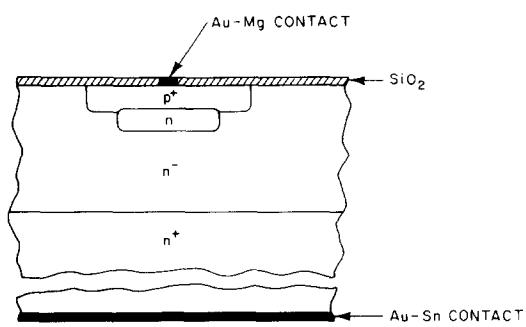

FIG. 1. Schematic illustration of the cross section of a planar guarded InP p-n junction diode.

 0003-6951/79/010074-03$00.50